C.P. No. 494
(20,477)
A.R.C. Technical Report

C.P. No. 494
(20,477)
A.R.C. Technical Report

MINISTRY OF AVIATION

AERONAUTICAL RESEARCH COUNCIL

CURRENT PAPERS

A Comparison between the Measured and Predicted Cooling Performance of an Internally Spanwise Ventilated Turbine Nozzle Blade.

by

R. I. Hodge

LONDON: HER MAJESTY'S STATIONERY OFFICE

1960

FIVE SHILLINGS NET

C.P. No.494

U.D.C. No. 621.438-226.3:621-712

Memorandum No. M.312

NATIONAL GAS TURBINE ESTABLISHMENT

July, 1958

A comparison between the measured and predicted cooling performance of an internally spanwise ventilated turbine nozzle blade

- by -

R. I. Hodge

SUMMARY

Profile average surface temperature at midspan and overall coolant pressure drop have been measured previously in a tunnel examination of a particular air-cooled turbine nozzle section. In this Memorandum values estimated using a procedure based on that described in Reference 1 are compared with those test results.

The agreement in the comparison is fairly good except for the effect of the gas/coolant temperature ratio. It is suspected that the internal heat transfer equation as adopted in Reference 1 is not applicable at the low Reynolds numbers of the coolant flows in this case.

CONTENTS

TABLE

APPENDIX

ILLUSTRATIONS

1.0 Introduction

In Reference 1 a method of estimating average surface temperatures and coolant pressure drops in air-cooled turbine blading is described. This method is applicable to internally spanwise-ventilated blading subjected to uniform gas conditions.

A cascade tunnel installed at this Establishment provides a satisfactory system for testing cooled blades of a representative turbine nozzle profile[2]. It has been used for cooling studies on a variety of blades, and the test results of one particular internally air-cooled blade are here compared with predictions based on the method given in Reference 1.

The test results are abstracted from Reference 3; they are those of the Wiggin extrusion profile A.1881/13 in the tip-shrouded mode of operation. This mode was selected as a distribution of the coolant which is unaffected by static pressure variation across the tip of the blade is an assumption implicit in the estimating procedure. The comparison is limited to perimeter-average surface temperatures at midspan only, and to overall coolant pressure drop.

2.0 Scope of the investigation

In making the comparison between estimated and test results it is preferable to modify the simple calculation outlined in Reference 1 to suit the tunnel conditions, rather than to correct the test results for certain effects not incorporated into the original estimating procedure. To this end the calculations incorporate modifying factors, based on tunnel measurements, to introduce the effects of radiation exchange between the test blade and its surrounds and of discrepancies between blade average surface temperature and mean temperature around the cooling duct perimeters.

To improve upon the accuracy of the basic calculation, the external heat transfer coefficient measured in Reference 2 was substituted for that embodied in the procedure of Reference 1. Smaller changes were also made in substituting actual blade dimensions for some representative values assumed in the original.

Optical measurement of the coolant channel areas and perimeters was of uncertain accuracy because of the difficulty in preparing a perpendicular cross-section without burrs or chamfers. Projection methods were unsuitable because of a slight variation in the hole geometry along the length of the section. Accordingly the area and perimeter of a single passage, equivalent in isothermal incompressible flow to the eleven channels was deduced from a series of hydraulic tests.

As before[3], 0.01 on the relative temperature scale was regarded as being a significant difference (or error).

2.1 Test range

The range of the calculations was as follows:-

Gas effective temperature T_g °K	Blade outlet Mach number M_2	Coolant ratio W_c/W_g	Temperature ratio T_g/T_{c1}	Blade outlet Reynolds number R_2
523	0.25	0.01	1.74	$2.4 \times 10^5 / 5.9 \times 10^5$
	0.45			
773		0.02	2.57	$1.4 \times 10^5 / 3.9 \times 10^5$
	0.65			
1023	0.85	0.03	3.43	$10^5 / 3.1 \times 10^5$

The coolant inlet temperature, T_{c1}, was assumed constant at 300°K.

3.0 Blade measurements

Reference 3 contains inspection dimensions from the tunnel, with the test blade in position. Certain minor discrepancies from the design were revealed, but these have been neglected here. The design values incorporated into the calculation are as follows:-

chord	c	=	0.186 ft
pitch	s	=	0.122 ft
span	L_s	=	0.378 ft
incidence		=	0°
blade inlet angle		=	0°
$\cos^{-1} o/s$		=	65°
blade perimeter	S_g	=	0.41 ft
platform surface area	A_R	=	1.52×10^{-2} ft^2
section length	L_p	=	0.408 ft

The actual position of the blade was similar to that of the test blade used to obtain the external heat transfer coefficients[2], so that these results should be applicable here.

3.1 Internal passage measurement

Because of the difficulty in obtaining a representative cross-section and suitably preparing it for the optical measurement of internal passage areas and perimeters, a single passage, equivalent in isothermal incompressible flow, was deduced from measurements of flow and pressure drop in a series of hydraulic tests. For this purpose the Fanning equation was adapted as follows -

$$P_{c1} - p_{c2} = \Delta p_c = \frac{\rho_c V_c^2}{2g} \left\{ \frac{1}{\alpha} + \left(1 + C_e\right) 4f \frac{L_p}{D_e} \right\} \quad \ldots \quad (1)$$

Accepting the assumptions that:-

(a) the effect of a sharp edged entry may be interpreted as an effective increase in friction factor, f, represented by $(1 + C_e)$. For the present blade geometry a value of C_e of 0.06 was selected[7] and assumed constant for turbulent flow. Variation in the value of C_e has but a relatively small influence on the final determination of passage dimensions. For laminar flow C_e was assumed to be zero.

(b) the empirical friction factor, f, is:-

in turbulent flow = $0.079\ R_c^{-0.25}$

in laminar flow = $16\ R_c^{-1}$

(c) the velocity distribution factor, α, is[6]:-

in turbulent flow $\approx$ 1

in laminar flow = 0.5

then the Fanning equation can be rewritten in terms of S_c and A_c and the measured W_c, Δp_c relation.

Figure 1 gives the isothermal incompressible relation between flow rate and pressure drop as measured using water at 15°C. From this, three conditions were selected, two from the laminar and one from the turbulent regimes:-

(i) in laminar flow W_c = 0.1 lb/sec, Δp_c = 32.5 lb/ft^2

(ii) in laminar flow W_c = 0.2 lb/sec, Δp_c = 84 lb/ft^2

(iii) in turbulent flow W_c = 1 lb/sec, Δp_c = 1.55×10^3 lb/ft^2

Substituting these values in the Fanning equation yields:-

(i) $S_c^2 = 1.04 \times 10^8\ A_c^3 - 1.59 \times 10^2\ A_c$

(ii) $S_c^2 = 1.345 \times 10^9\ A_c^3 - 3.18 \times 10^2\ A_c$

(iii) $S_c^{1.25} = 1.550 \times 10^9\ A_c^3 - 2.50 \times 10^2\ A_c$

These three relations are plotted in Figure 2. There are no unique values which satisfy all three curves. This must be attributed to slight errors in the assumed values for α and C_e in the Fanning equation. The nearest common values were selected as:-

$A_c = 7.8 \times 10^{-4}$ ft^2

$S_c = 0.615$ ft

The corresponding total measurements from enlargements of end-view photographs (Figure 5 is traced from the root view) were rather different. They were:-

$$A_c = 8.7 \times 10^{-4} \text{ and } 9 \times 10^{-4} \text{ ft}^2$$

$$S_c = 0.549 \text{ and } 0.548 \text{ ft}$$

respectively from root and tip photographs.

The apparent dimensions from the hydraulic tests were selected for incorporation into the calculations, to be utilised in equations of the same nature as those used in their deduction.

4.0 Calculations

4.1 Blade and coolant temperatures

The calculations were based on the approximate method of Reference 1, in which the parameter $X = \frac{h_c S_c}{h_g S_g}$ is assumed constant along the span, the heat transfer coefficients being evaluated at the midspan gas and coolant conditions.

The coolant heat transfer equation quoted in Reference 1 was adopted:-

$$\overline{Nu}_c = 0.034 \; Pr^{0.4} \left(\frac{L_p}{D_c}\right)^{-0.1} \left(\frac{T}{T_{cm}}\right)^{0.8} \left(\frac{\overline{T}_{cm}}{\overline{T}_{bm}}\right)^{0.55} \quad \ldots \quad (2)$$

The gas to blade heat transfer coefficients obtaining in this tunnel (in the absence of radiation) have previously been reported[2], and the experimental extrapolation to the temperature ratio $T_g/T_b = 1$ is reproduced in Figure 4. The design rule from Reference 1 is compared with these test results in the same figure and is shown to be generally low, the error varying between 5 per cent and 19 per cent at the extremes of the Reynolds number range 10^5 to 5.8×10^5. To improve upon the accuracy of the prediction the following power approximations to the test results were introduced into the calculation:-

(a) $R_2 < 2 \times 10^5$

$$\overline{Nu}_g = 1.134 \; R_2^{0.463} \left(\frac{T_g}{\overline{T}_{bm}}\right)^{-0.16} \quad \ldots \quad \ldots \quad (3)$$

(b) $R_2 > 2 \times 10^5$

$$\overline{Nu}_g' = 0.055 \; R_2^{0.715} \left(\frac{T_g}{\overline{T}_{bm}}\right)^{-0.16} \quad \ldots \quad \ldots \quad (4)$$

Introducing the design external dimensions quoted in Section 3.0 and the experimentally determined internal measurements from 3.1 gives the following parameters:-

$$\overline{X} = 0.353\,\phi^{0.8}\,R_2^{0.337}\left(\overline{T}_{cm}/T_g\right)^{0.824}\left(T_g/\overline{T}_{bm}\right)^{0.71} \quad \ldots\ \ldots\ \ldots \quad (5)$$

$$\overline{X}' = 17.6\,\phi^{0.8}\,R_2^{0.085}\left(\overline{T}_{cm}/T_g\right)^{0.824}\left(T_g/\overline{T}_{bm}\right)^{0.71} \quad \ldots\ \ldots\ \ldots \quad (6)$$

and

$$\overline{K} = 13.93\,\phi^{-1}\,R_2^{-0.587}\left(T_g/\overline{T}_{bm}\right)^{-0.16}\left(T_g/\overline{T}_{cm}\right)^{0.15}\frac{\overline{X}}{1+\overline{X}}\left(\frac{\ell + 0.037}{0.375}\right) \quad \ldots (7)$$

$$\overline{K}' = 0.675\,\phi^{-1}\,R_2^{-0.285}\left(T_g/\overline{T}_{bm}\right)^{-0.16}\left(T_g/\overline{T}_{cm}\right)^{0.15}\frac{\overline{X}'}{1+\overline{X}'}\left(\frac{\ell + 0.037}{0.375}\right) \quad \ldots (8)$$

where $\overline{X}$ and $\overline{K}$ are applied if R_2 is less than 2×10^5 and $\overline{X}'$ and $\overline{K}'$ at Reynolds numbers between 2×10^5 and 10^6.

Following Reference 1, the blade relative temperatures and coolant relative temperatures at midspan were calculated from:-

$$\left(\overline{T}_{bm} - T_{c1}\right)/\left(T_g - T_{c1}\right) = 1 - \frac{\overline{X}}{1+\overline{X}}\,e^{-\overline{K}_m} \quad \ldots\ \ldots\ \ldots \quad (9)$$

and

$$\left(\overline{T}_{cm} - T_{c1}\right)/\left(T_g - T_{c1}\right) = 1 - e^{-\overline{K}_m} \quad \ldots\ \ldots\ \ldots \quad (10)$$

where $\overline{K}_m$ signifies the substitution of $\ell = \frac{L_s}{2}$ into $\overline{K}$, and where prime values of $\overline{X}$ and $\overline{K}$ are used when applicable. The corresponding temperatures are listed in Columns 1 and 2 of Table I.

4.2 Modification to basic calculation

Having obtained first approximation values of blade and coolant midspan relative temperatures as above, corrections were made to the calculation to introduce the effects

(a) of radiant heat exchange between the test blade and its surrounds, and

(b) of variation of metal temperature within the core of the blade.

4.2.1 Correction for radiation exchange

The tunnel walls and fixed blade surfaces were at temperatures differing from those measured on the test blade surfaces: to simplify radiation calculation this effect was simulated by stipulating an envelope around the test blade, at a distance of one pitch, whose inner surface temperature was uniform at some value $\overline{T}_{wr}$. This radiation effective temperature may be deduced from the temperatures and geometry of the individual surround surfaces as follows:-

$$T_{wr} = \sqrt[4]{\sum \frac{\left(\oint_{LE}^{TE} f_r \cdot dA_g\right) s^2 \cdot T_W^4}{A_g \oint_{LE}^{TE} y^2 \cdot dA_g}} \qquad \ldots \ldots \ldots \quad (11)$$

where f_r = configuration factor between surround and test blade

y = distance between the origin of surround and test blade

T_W = surround temperature

s = blade pitch

$A_g = L_s . S_g$ = profile surface area.

The calculation was further simplified by neglecting radiation originating or incident at cone angles greater than 30°, measured from the perpendicular to the surface under consideration: furthermore all radiation within these conical limits was assumed to be of uniform intensity. Areas of influence, a_g, on the surface of the test blade were then measured considering the surrounds as emitters, and the distances between emitters and target centres were assumed to be equal to the root mean square values over the surfaces.

Thus

$$\overline{T}_{wr} \simeq \sqrt[4]{\sum \frac{a_g s^2 T_W^4}{A_g y^2}} \qquad \ldots \ldots \ldots \quad (12)$$

This effective temperature, which is plotted in Figure 5, was produced from a survey of the measured fixed blade surface temperatures and estimated tunnel wall surface temperatures over the test range.

Positive external radiant heat exchange was regarded as supplementing the convective heat transfer coefficient. The total flow of heat into the blade then becomes:-

$$h_g A_g (T_g - \overline{T}_{bm}) + A_g \cdot 2.805 \times 10^{-12} (\overline{T}_{wr}^4 - T_{bm}^4). \qquad \ldots \ldots \quad (13)$$

If this is equated to $h_{gr} A_g (T_g - \overline{T}_{bm})$, it may be used to define a corrected value of heat transfer coefficient which can be introduced into the calculations in place of h_g.

$$h_{gr} = h_g \left(1 + \frac{2.803 \times 10^{-12} \left(\overline{T}_{wr}^4 - T_{bm}^4 \right)}{h_g \left(T_g - \overline{T}_{bm} \right)} \right) = \frac{h_g}{\eta_r} \quad .. \quad (14)$$

The parameter $\overline{X}$ may then be corrected:-

$$\overline{X}_r = \eta_r \overline{X} \qquad \ldots \ldots \ldots \quad (15)$$

and $\overline{K}$:-

$$\overline{K}_r = \frac{\dfrac{\overline{X}_r}{1 + \overline{X}_r}}{\dfrac{\overline{X}}{1 + \overline{X}}} \cdot \frac{\overline{K}}{\eta_r} \cdot \qquad \ldots \ldots \ldots \quad (16)$$

When the radiation envelope temperatures of Figure 5 are converted to the relative scale, $\overline{T}_{wr} - T_{c1} / T_g - T_{c1}$, using the relevant values of gas effective temperature, they reduce to a unique relation with gas Reynolds number. This line is given in Figure 7(a), where it may be compared with the first approximation blade midspan surface temperatures. The radiation exchange at coolant flows 0.01 and 0.02 serves to reduce the convective heat transfer, particularly at low gas and coolant flows. Over the upper half of the Reynolds number range radiation supplements gas to blade convection when 3 per cent coolant is passed through the ventilating system.

4.2.2 Correction for variable cooling passage wall temperature

The distribution of the ventilating ducts in this profile is such that the flow of heat into the core of the blade is restricted to some extent by the presence of the cooling passages. Consequently the core side surfaces of the cooling passages were at lower temperatures than the profile perimeter sides, during the tests. If it is assumed that the cooling heat transfer coefficient is everywhere uniform, then the heat flowing to the coolant per unit area of passage surface would be proportional to $\overline{T}_{bc} - \overline{T}_{cm}$ from the core, and proportional to $\overline{T}_{bm} - \overline{T}_{cm}$ from the blade outside surface.

Figure 6 (taken from Reference 3, Figure 17 (a)) gives the midspan core temperatures over the test range; these were taken to be effective at the core side surfaces of the ventilating passages, which area amounted to roughly one half of the total passage surface. The first approximation midspan coolant temperatures provided the $\overline{T}_{cm}$ term. The calculation was then corrected for this partial insulation effect by multiplying the average inside heat transfer coefficient by a modifying factor, η_{sc}:-

$$\eta_{sc} h_c = \frac{h_c}{2} \left[1 + \overline{T}_{bc} - \overline{T}_{cm} / \overline{T}_{bm} - \overline{T}_{cm} \right] \qquad \ldots \ldots \ldots \quad (17)$$

i.e.

$$\eta_{sc} = \frac{1}{2}\left[1 + \left[\frac{\left(\overline{T}_{bc} - T_{c1}/T_g - T_{c1}\right) - \left(\overline{T}_{cm} - T_{c1}/T_g - T_{c1}\right)}{\left(\overline{T}_{bm} - \overline{T}_{c1}/T_g - T_{c1}\right) - \left(\overline{T}_{cm} - T_{c1}/T_g - T_{c1}\right)}\right]\right] \quad \ldots \quad (17a)$$

The variation of η_{sc} over the test range is shown in Figure 7(b). The temperature drop from blade surface to core is increased as the heat flow into the blade is increased, i.e. as the relative blade surface temperature is reduced. This produces a pattern of η_{sc} similar in trend to that of the blade temperature with respect to the parameters Reynolds number, coolant flow and temperature ratio.

In Reference 1 the effectiveness of the geometrical cooling arrangement is denoted by a parameter $Z = \frac{\left(S_c/c\right)^{1.2}}{A_c/c}$. If it is desired to refer to an effective reduction of this geometrical Z-factor due to the core insulation, the above modifying factor may be applied as (η_{sc}) Z.

The parameter $\overline{X}$ may then be corrected:-

$$\overline{X}_s = \eta_{sc}\,\overline{X} \quad \ldots \quad \ldots \quad \ldots \quad (18)$$

and $\overline{K}$:-

$$\overline{K}_s = \frac{\dfrac{\overline{X}_s}{1 + \overline{X}_s}}{\dfrac{\overline{X}}{1 + \overline{X}}}\,\overline{K}\,. \quad \ldots \quad \ldots \quad \ldots \quad (19)$$

4.2.3 Combined corrections

The two corrections, described in the preceding sections, are incorporated together in the calculation of midspan blade and coolant relative temperatures given in Columns 3 and 4 of Table I In these estimates the following parameters were used:-

$$\overline{X}_c = \eta_{sc}\,\eta_r\,\overline{X} \quad \ldots \quad \ldots \quad \ldots \quad (20)$$

$$\overline{K}_{mc} = \frac{\dfrac{\overline{X}_c}{1 + \overline{X}_c}}{\dfrac{\overline{X}}{1 + \overline{X}}}\,\frac{\overline{K}_m}{\eta_r} \quad \ldots \quad \ldots \quad \ldots \quad (21)$$

Prime values were used when applicable.

4.3 Coolant pressure drop

Using the corrected values of $\bar{X}_c$ and $\bar{K}_c$, but substituting $\ell = L_s$ to give $\bar{K}_{2c}$, the coolant outlet temperature $\bar{T}_{c2}$ was calculated. From this, by an iterative method, the outlet Mach number $\bar{M}_{c2}$ was estimated:-

$$\bar{M}_{c2} = 0.0892\ \phi\ R_2\ \mu_g \sqrt{t_{c2}} . \qquad \ldots\ \ldots\ \ldots\ (22)$$

This is listed in Column 6 of Table I.

The outlet Mach numbers are sufficiently low that the simplified pressure drop calculation, laid out in Reference 1, may be used. This gives, when the blade and cascade design dimensions are incorporated:-

$$\frac{P_{c2} - P_{c2}}{\frac{1}{2}\rho_g\ V_{g2}^2} = 6.18 \times 10^3\ \phi^2\ \bar{T}_{c2}/T_g \qquad \ldots\ \ldots\ \ldots\ (23)$$

and

$$\frac{P_{c1} - P_{c2}}{\frac{1}{2}\rho_g\ V_{g2}^2} = 2.12 \times 10^4\ R_2^{-0.25} \left(\bar{T}_{cm}/T_g\right)^{1.155}\ \phi^{1.75} \left\{0.816 + 0.412\left(\bar{T}_{bm}/T_{cm} - 1\right)\right\}$$

(turbulent flow)

$$\ldots\ \ldots\ \ldots\ (24)$$

or

$$5.74 \times 10^6\ R_2^{-1} \left(\bar{T}_{cm}/T_g\right)^{1.62}\ \phi \left(\bar{T}_{bm}/\bar{T}_{cm}\right)^{0.45} \left\{0.816 + 0.412\left(\bar{T}_{bm}/T_{cm} - 1\right)\right\}$$

(laminar flow).

$$\ldots\ \ldots\ \ldots\ (25)$$

The coolant outlet velocity head and channel total pressure drop, evaluated with $\bar{T}_{bm}$, $\bar{T}_{cm}$ and $\bar{T}_{c2}$ deduced from Columns 3, 4 and 5, are listed separately and summed in Columns 7, 8 and 9 respectively, in Table I.

5.0 Comparison with test results

5.1 Midspan perimeter-average surface temperatures

The relevant test results, from Reference 2, are compared with the estimated values, from Column 3 of Table I, in Figure 8. Although the general trend with respect to Reynolds number at all coolant ratios appears similar in both cases, the spread of the curves due to temperature ratio effects, which is strongly marked in the test results, is under-emphasised by the estimating process. The curves estimated for a temperature ratio $T_g/T_{c1} = 1.75$ are in best agreement with their corresponding test values.

The variables can be separately examined in Figures 9 and 10.

In the former the relative temperatures are plotted against temperature ratio logarithmically, forming groups of straight lines when considered at constant coolant flow ratio or at constant Reynolds number. In both cases surface temperature is proportional to positive power functions of the temperature ratio, the exponent increasing both with increasing coolant ratio and increasing Reynolds number. Within the range of the investigation the test results gave temperature ratio exponents between 0.064 and 0.254, whereas within the same range the calculated effect varies between 0.022 and 0.07.

By extrapolating the lines of Figure 9, plots of surface temperature for unity temperature ratio may be obtained. Such a plot is presented in Figure 10. This discloses discrepancies between estimate and test in the relation between surface relative temperature and Reynolds number. At low Reynolds numbers the two cases agree at all coolant ratios, but at higher Reynolds numbers the estimated values are considerably higher than measured.

5.2 Coolant pressure drop

The estimated channel total pressure drop (Column 8 of Table I) and overall pressure drop (Column 9) are compared with the measured pressure drop in Figure 11. In general, the test results lie midway between the estimated drops at outlet Reynolds number = 2×10^5, but at 4×10^5 are nearer the estimated overall pressure drop. This could at first sight be ascribed to some velocity head recovery in the outlet manifold in the experimental arrangement.

In Figure 12 the coolant pressure drops, (test and estimated overall), are plotted logarithmically. The change in slope between the two modes of flow will be observed. A limit is drawn in on each coolant flow ratio group marking the points at which the coolant channel Reynolds number, calculated at estimated midspan conditions, has the value 2,300. Also included in Figure 12 are lines at temperature ratio $T_g/T_{c1} \rightarrow 1$. These apply to the turbulent flow points only, and were obtained by extrapolation on a logarithmic plot of pressure drop versus temperature ratio (Figure 13).

Over the range of Reynolds number within which the cooling flow is turbulent, the agreement between the unity temperature ratio plots of estimated overall and measured pressure drop is fairly good: at a coolant flow ratio of 0.01 the estimated line lies about 8 per cent below the test results; at $W_c/W_g = 0.02$ the estimate is some 4 to 5 per cent high and in the highest coolant flow group the plots lie well within 1 per cent of each other. As many of the test readings in the 1 per cent coolant flow group of results were of very low magnitude, it is thought that the explanation of the 8 per cent discrepancy between estimated and measured pressure drops lies within the bounds of probable experimental inaccuracy. The slopes of the plots also agree fairly well; here analytical inaccuracy could account for the small differences observed.

Concerning the relation between pressure drop and temperature ratio, it will be observed that Figure 13 displays some differences between the estimated and measured results. The slope of the test results shows a stronger dependence upon coolant flow ratio, varying from -0.25 at 1 per cent flow to -0.48 at 3 per cent, whereas the estimated variation is from -0.29 to -0.40 within the same limits.

6.0 Discussion

The estimate of midspan profile perimeter-mean temperature is considerably different from the test results, particularly in the matter of temperature ratio effect. When the blade relative temperature is expressed as a power function of temperature ratio the estimated exponents are approximately one third of the values derived from the test results. The various factors which could contribute to this discrepancy are:-

(a) the viscosity-temperature and conductivity-temperature relations assumed in the design procedure,

(b) the gas/blade temperature ratio $\left(T_g/\overline{T}_b\right)$ effect introduced into the design procedure from Reference 2,

(c) the coolant/blade temperature ratio $\left(\overline{T}_c/\overline{T}_b\right)$ effect incorporated in the design procedure and derived from the work described in Reference 4.

There is some disagreement between different authorities on the relationship in the temperature-dependent physical properties of air, particularly in the case of thermal conductivity. The data collected in Reference 5 yields, for example, viscosity $\propto T^{0.67}$, conductivity $\propto T^{0.86}$; the values used in the estimating procedure were those given in the original[1], which were viscosity $\propto T^{0.62}$ and conductivity $\propto T^{0.77}$. A simple analysis indicates that adoption of the Reference 5 data would increase the temperature ratio effect in the estimates by approximately 40 per cent.

The gas/blade temperature ratio effect (b) was determined experimentally on this particular profile[2], and is considered accurate to within ±1 per cent, up to the value 2.

The coolant/blade temperature ratio effect (c) adopted in the estimating procedure should properly be limited to coolant Reynolds numbers greater than 10^4: the bulk of the flows considered lie considerably below this value. The data presented in Reference 4 show a very much enhanced but irregular temperature ratio effect at these lower flows. An increase in the exponent of the $\overline{T}_c/\overline{T}_b$ term on the coolant side obviously increases the overall temperature ratio $\left(T_g/T_{c1}\right)$ effect. It is suspected that this is probably the major cause of the discrepancies observed. However, the adoption of a variable exponent in the $T_c/\overline{T}_b$ term considerably complicates the estimating procedure, and consequently has not been explored.

When temperature ratio effects are taken out, the estimated mean temperatures are much nearer the measured values, although still outside the significant difference over most of the test range. The greatest discrepancy is about 0.05. The estimated mean temperatures are generally greater than measured; the discrepancy increases with gas outlet Reynolds number but not with coolant flow ratio, suggesting that the external Nusselt number - Reynolds number relation used has over-emphasised heat transfer coefficients at high Reynolds numbers. This effect may be traced to the non-uniform distribution of perimeter-average Nusselt number along the span of the test blade, predicted in Reference 2. Local

discrepancies in the perimeter-average coefficient from the whole surface-average Nusselt number were themselves proportional to Reynolds number. The midspan station was a location where the local values were generally low, falling to +6 per cent below the average value at high flows with one particular selection of combustion system. As the midspan deficit from the surface average Nusselt number - Reynolds number relation was complex and as the heat transfer over the rest of the span enters into the determination of the midspan surface temperatures by spanwise conduction and in the coolant temperature rise, the known effect was ignored and the calculation carried out on the assumption that surface average values were adequately representative.

The Mach number of the cooling flow near the outlet of the channels does not exceed 0.6, and is generally below 0.4. The simplified pressure drop calculation gives values which are in reasonable agreement with the test results. When temperature ratio effects are eliminated the calculated overall pressure drop, which includes channel outlet velocity head, agrees fairly well with the test results. However, the variation in the temperature ratio effect is underestimated in the calculations: this is probably a reflection of the discrepancies in the midspan surface temperature comparison.

7.0 Conclusions

Two additional features not included in the original have been added to the general design procedure given in Reference 1. These are:-

(a) radiation heat exchange between blade and surrounds,

(b) the debasing of the effectiveness of the ventilating system, to allow for the variation of temperature around the cooling duct perimeters.

In the particular cascade test arrangement which was investigated the first feature had a small effect on blade surface temperature, amounting generally to an additional cooling which lowered the midspan average surface temperature by not more than 0.03 on the relative scale. The second feature, which is inherent in the blade design and is not a tunnel peculiarity, suggested that at high rates of heat flow through the blade the effective value of the Z factor was only some 80 per cent of the geometrical value: as a result of this correction the estimated average surface temperatures rose by about 0.06 on the relative scale.

When the final calculated blade midspan average surface temperatures, which included the above features and which were also based on actual measured values of gas to blade heat transfer coefficients, were compared with the test information, it appeared that:-

(a) the predictions were fairly accurate as far as Reynolds numbers and coolant flow effects were concerned,

(b) the temperature ratio $\left({}^{T_g}/_{T_{c1}}\right)$ effect was underemphasised in the estimating procedure.

The latter discrepancy amounted to the exponent in the $\left({}^{T_g}/_{T_{c1}}\right)$ term being estimated at about one third of the value indicated in the test results.

It is suspected that the major reason for the discrepancy is the adoption of $\left(\overline{T}_{cm}/\overline{T}_{b}\right)^{0.55}$ in the coolant heat transfer equation (Section 4.1): it appears that at the values of coolant Reynolds number experienced here the exponent should be considerably greater. It is also possible that there is a second contributing cause: the choice of temperature relationship for the air viscosity and conductivity is not commonly agreed, particularly in the latter case, and it may be that the values selected in the analysis in Reference 1 are not accurate.

The comparison between measured and estimated coolant pressure drop shows good agreement except in the matter of temperature ratio effect. This is thought to be a reflection of the discrepancies in the surface temperature comparison.

REFERENCES

No.	Author(s)	Title, etc.
1	D. G. Ainley	Internal air-cooling for turbine blades. A general design survey. A.R.C. R & M No. 3013. 1957.
2	R. I. Hodge	A turbine nozzle cascade for cooling studies. Part I - The measurement of mean Nusselt numbers on the blade surface. C.P.492. May, 1958.
3	R. I. Hodge	The cooling performance of two extruded turbine nozzle profiles. C.P.495. July, 1958.
4	L. V. Humble W. H. Lowdermilk L. G. Desmon	Measurements of average heat transfer and friction coefficients for subsonic flow of air in smooth tubes at high surface and fluid temperatures. N.A.C.A. Report No. 1020. 1951.
5	J. H. Keenan J. Kaye	Gas tables. John Wiley & Sons, New York. 1948.
6	W. H. McAdams	Heat transmission. McGraw-Hill (2nd edition) 1942.
7	W. M. Kays	A summary of experiments and analysis for gas flow heat transfer and friction in circular tubes. Technical Report No. 22; Department of Mechanical Engineering; Stanford University, California. 1954.

TABLE I(a)

Calculated performance

Gas temp. T_g °K	Blade outlet		Coolant ratio W_c/W_g	Cooling passage Reynolds number R_{cm}	First approx.	
	Mach number M_2	Reynolds number R_2			Midspan blade rel. temp. (1)	Midspan cool. rel. temp. (2)
523	0.25	2.37×10^5	0.01	1.86×10^5	0.717	0.478
			0.02	3.92	0.557	0.330
			0.03	6.05	0.456	0.255
	0.45	3.04	0.01	2.41	0.708	0.451
			0.02	5.05	0.543	0.314
			0.03	7.80	0.442	0.241
	0.65	4.41	0.01	3.53	0.688	0.421
			0.02	7.41	0.522	0.288
			0.03	11.41	0.424	0.221
	0.85	5.89	0.01	4.75	0.688	0.393
			0.02	9.97	0.506	0.269
			0.03	15.34	0.408	0.204
773	0.25	1.43	0.01	1.20	0.760	0.512
			0.02	2.60	0.606	0.365
			0.03	4.11	0.507	0.286
	0.45	1.85	0.01	1.57	0.741	0.484
			0.02	3.42	0.583	0.342
			0.03	5.40	0.483	0.265
	0.65	2.74	0.01	2.37	0.721	0.451
			0.02	5.15	0.561	0.315
			0.03	8.11	0.462	0.244
	0.85	3.94	0.01	3.47	0.704	0.420
			0.02	7.52	0.543	0.291
			0.03	11.82	0.444	0.224
1023	0.25	1.04	0.01	0.89	0.794	0.540
			0.02	1.99	0.638	0.385
			0.03	3.16	0.552	0.316
	0.45	1.33	0.01	1.15	0.772	0.526
			0.02	2.56	0.623	0.377
			0.03	4.10	0.528	0.296
	0.65	1.95	0.01	1.75	0.741	0.473
			0.02	3.89	0.588	0.333
			0.03	6.21	0.491	0.260
	0.85	3.12	0.01	2.88	0.722	0.453
			0.02	6.38	0.565	0.302
			0.03	10.19	0.467	0.234

FIG. 1.

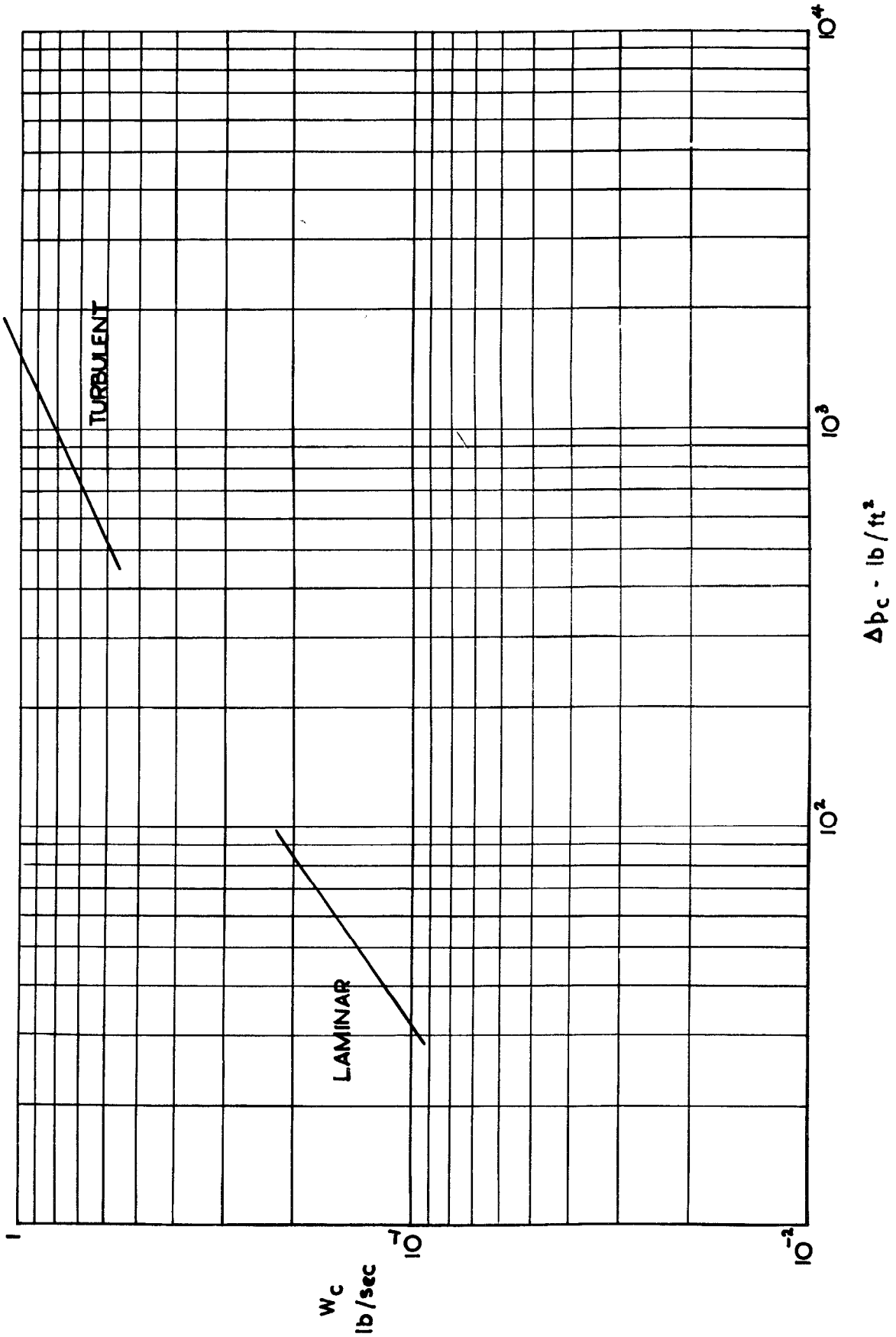

HYDRAULIC FLOW IN COOLING CHANNELS

FIG. 2.

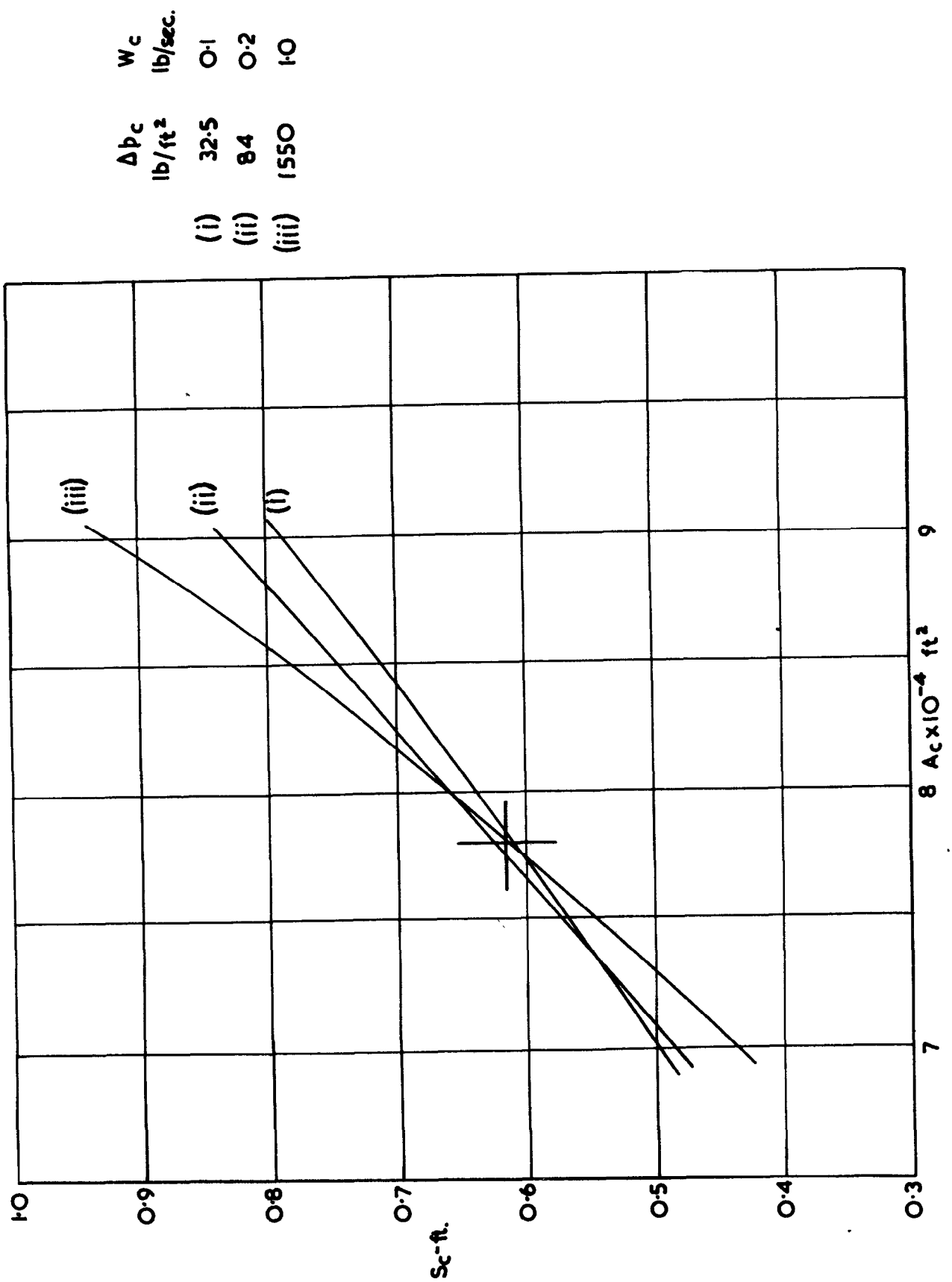

A_c-S_c RELATION IN LAMINAR AND TURBULENT FLOW

FIG. 3.

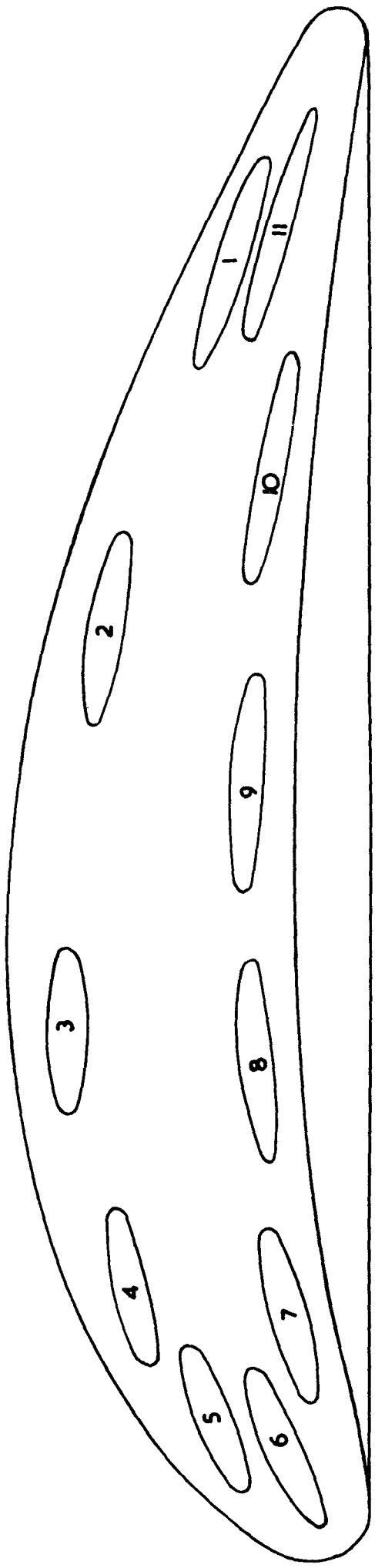

PROFILE

FIG. 4.

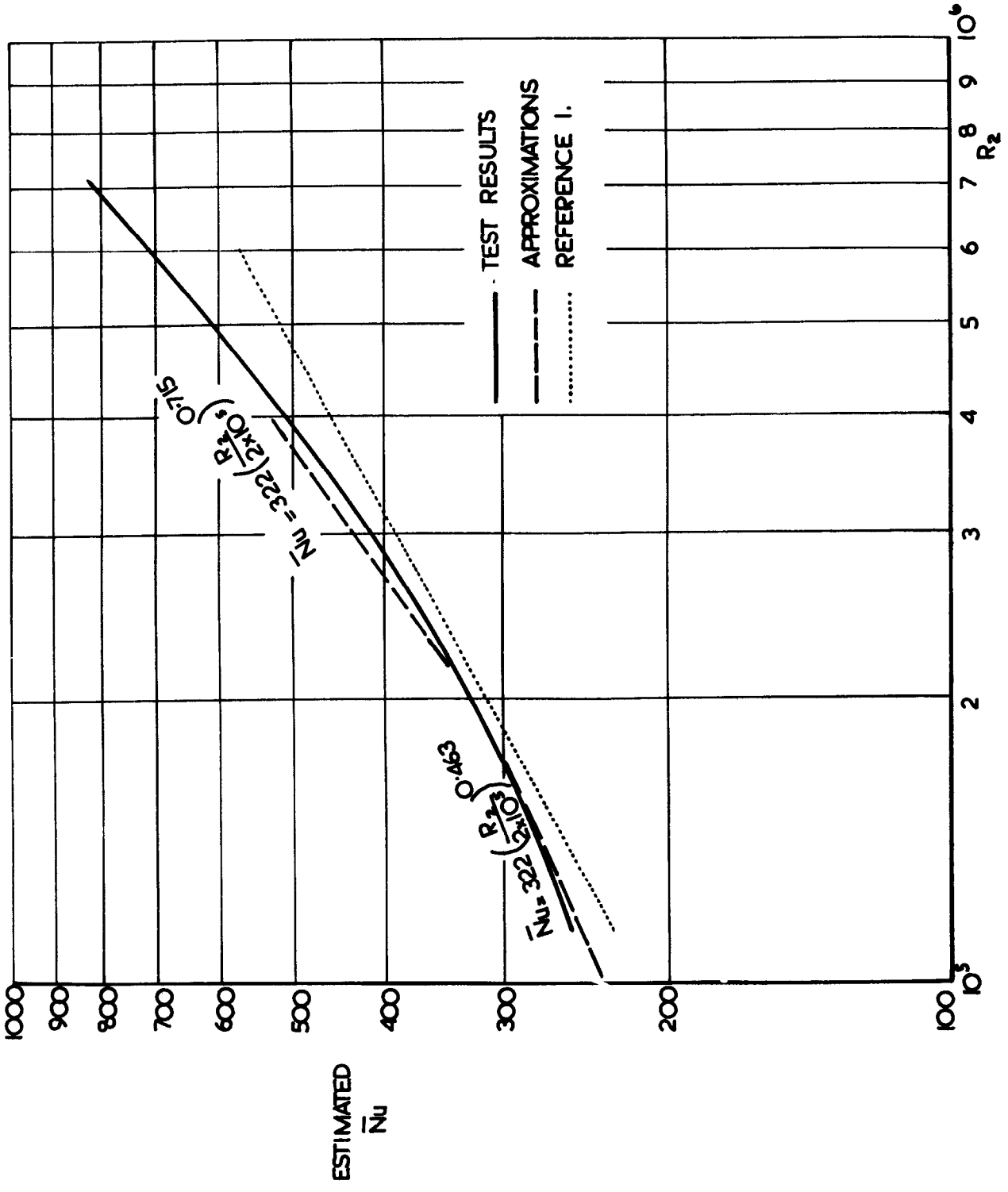

HEAT TRANSFER COEFFICIENT FOR $T_g/T_b = 1$

FIG.5.

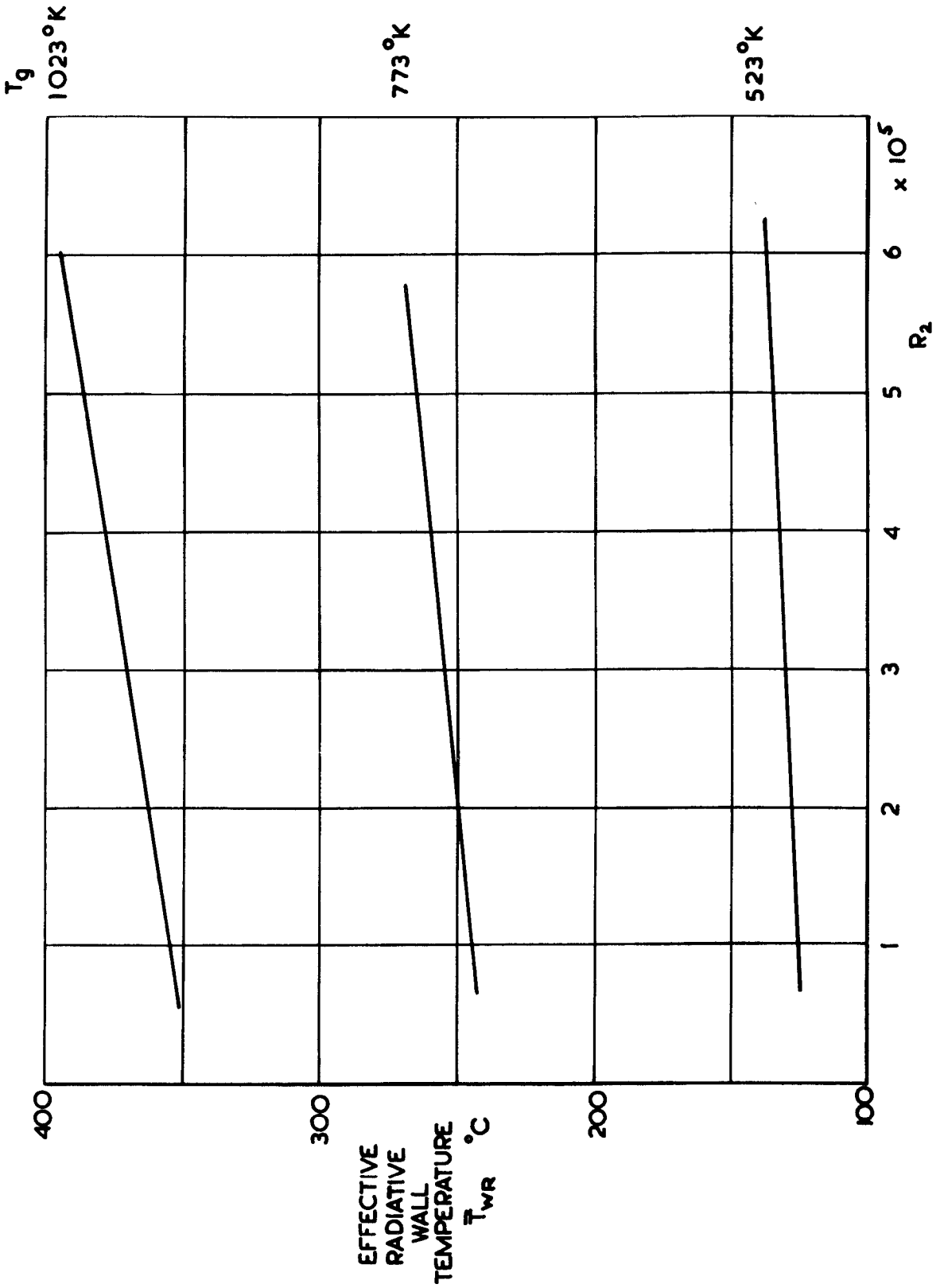

RADIATION ENVELOPE TEMPERATURE

FIG. 6

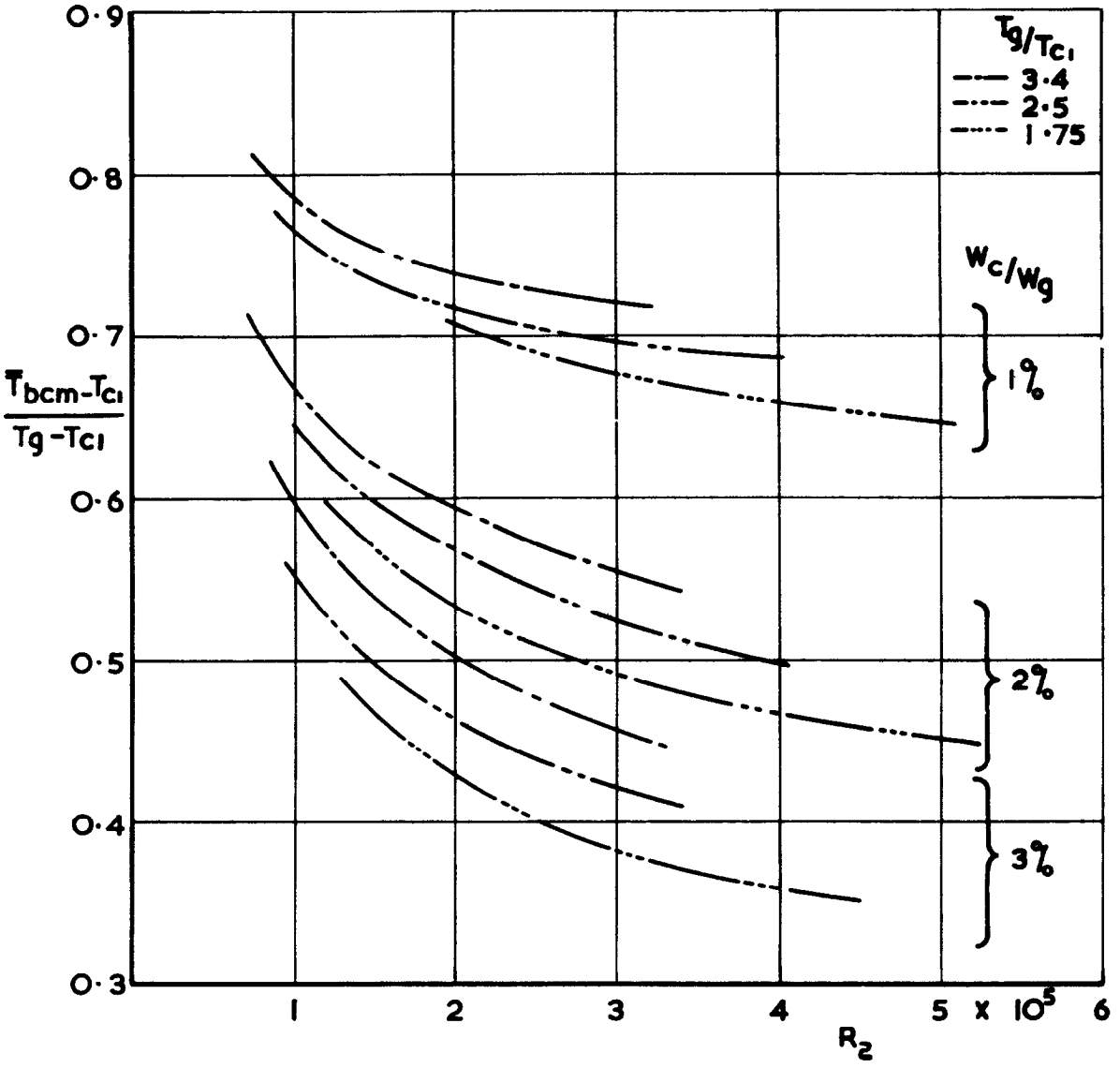

CORE TEMPERATURE AT MIDSPAN.

FIG. 7.

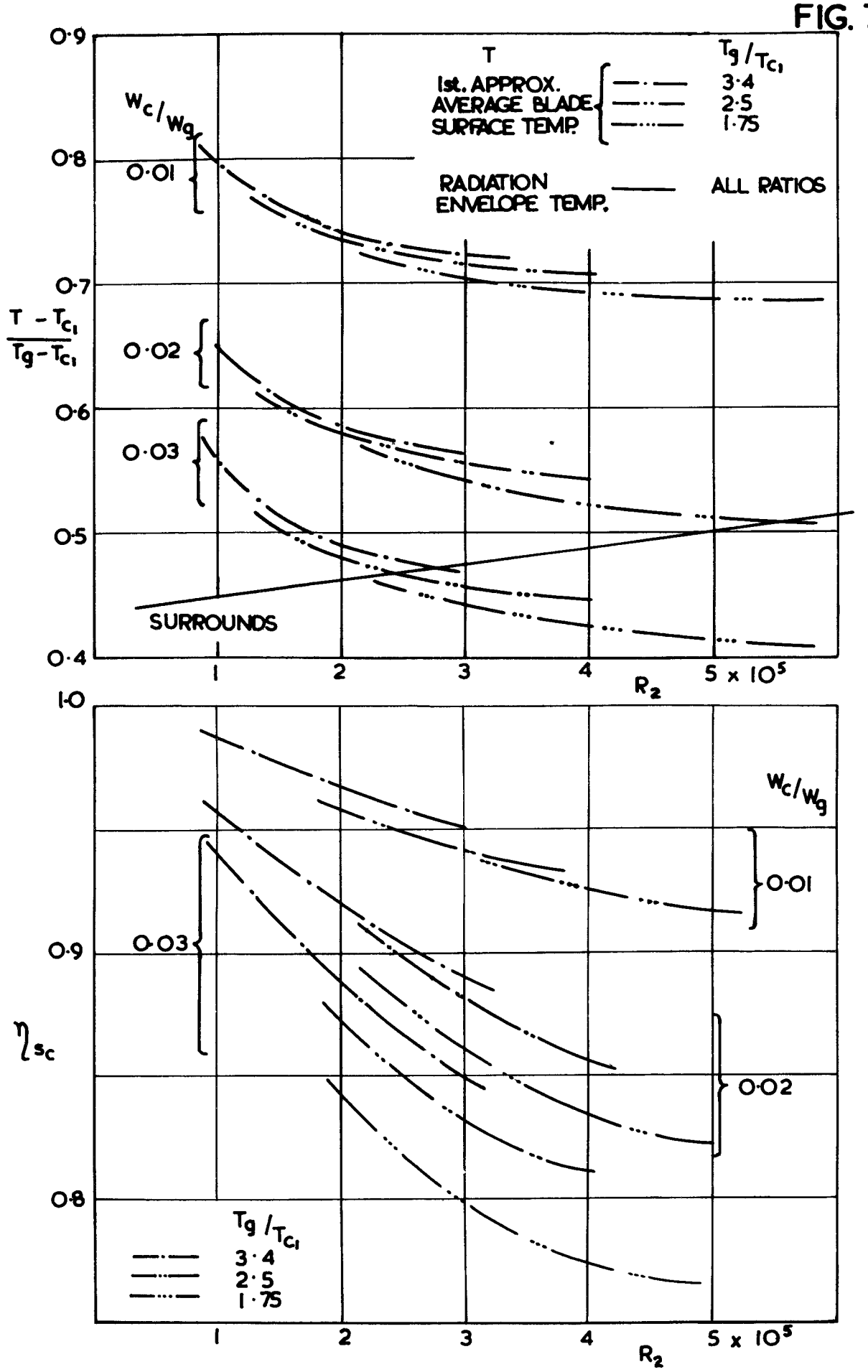

FIRST APPROXIMATION SURFACE TEMPERATURES AND CORRECTION FACTORS

FIG.8.

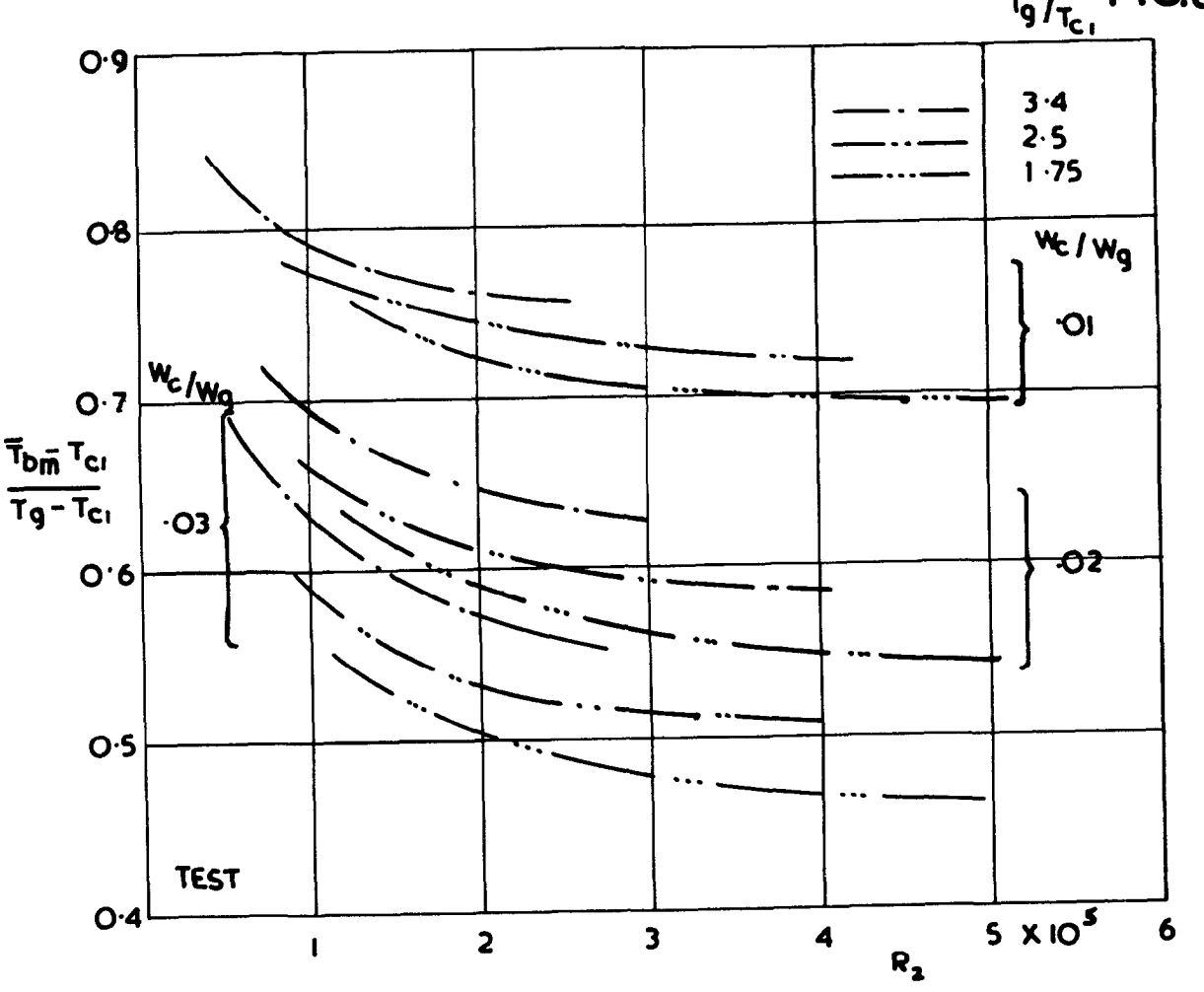

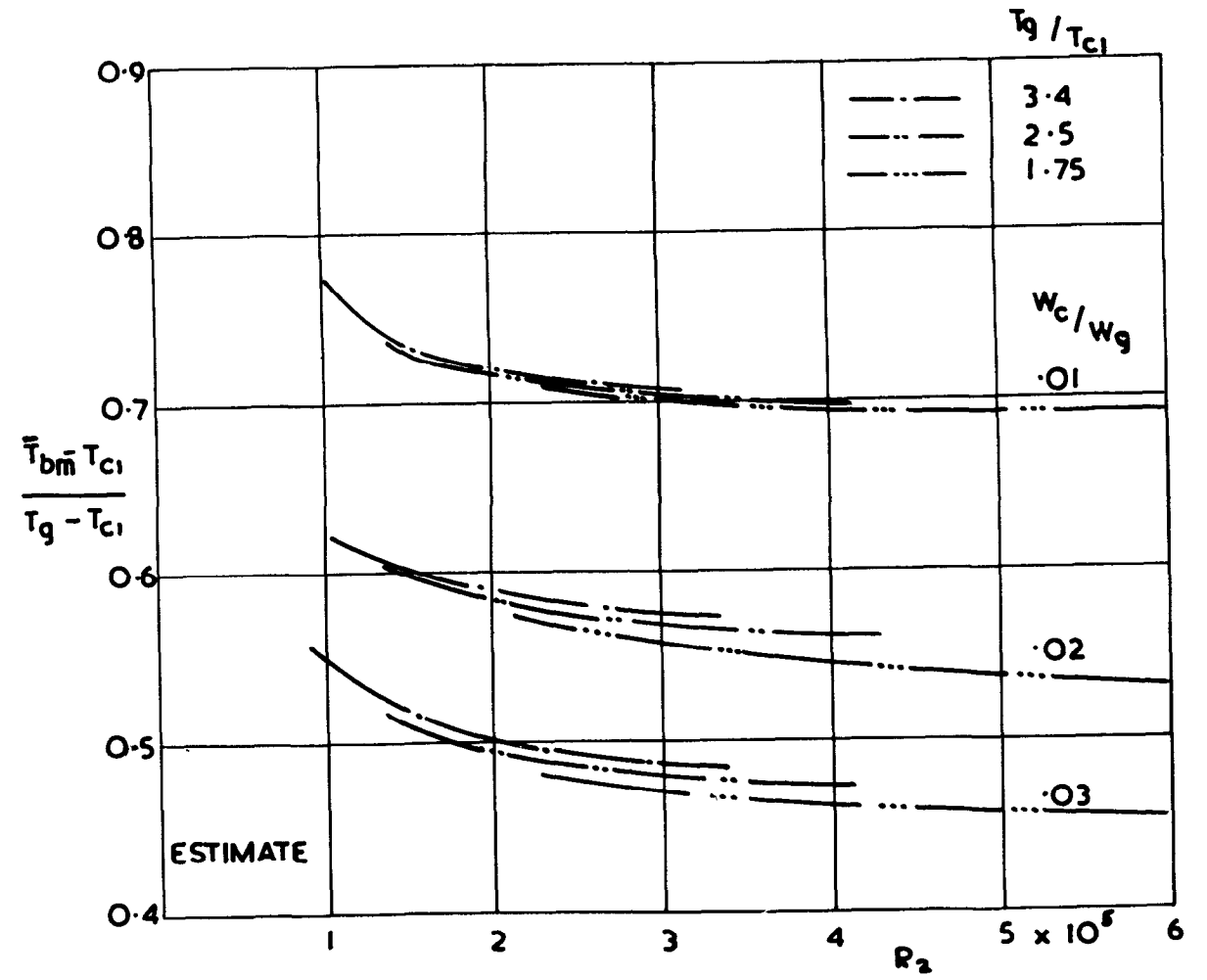

MIDSPAN MEAN SURFACE TEMPERATURES

FIG.9.

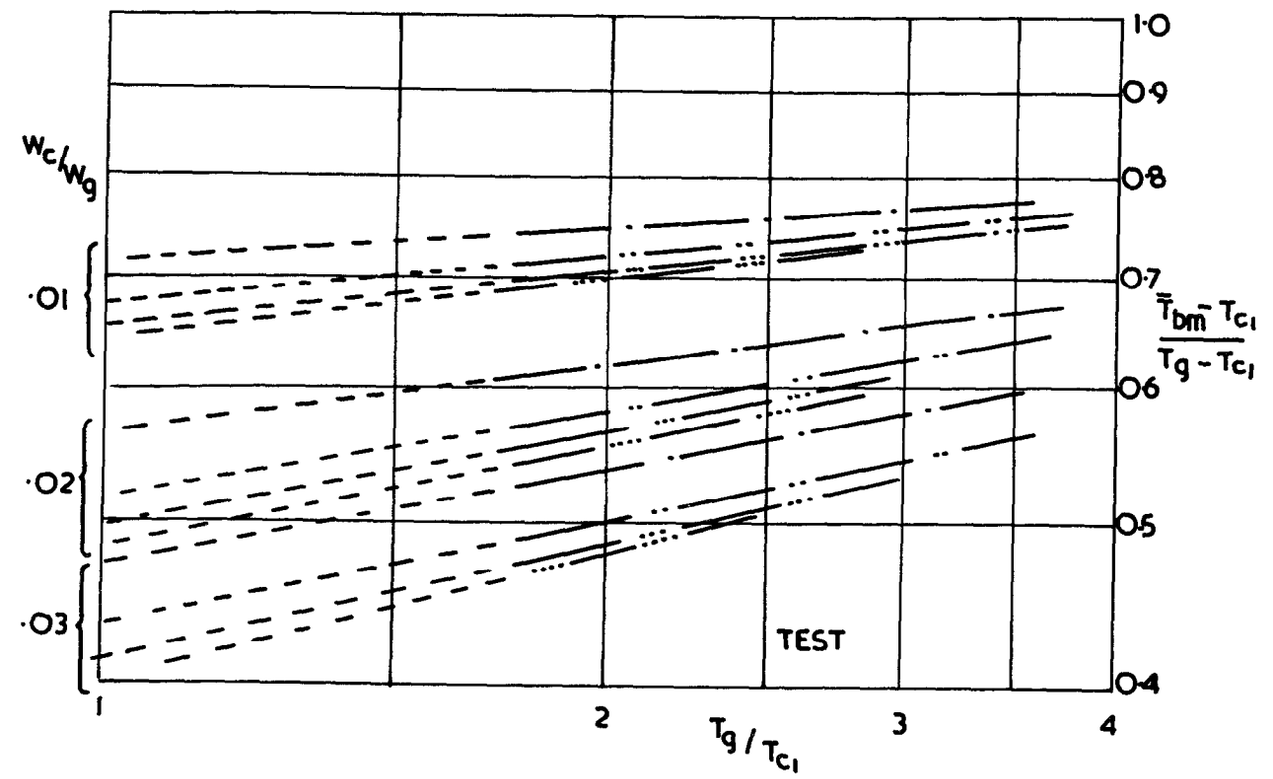

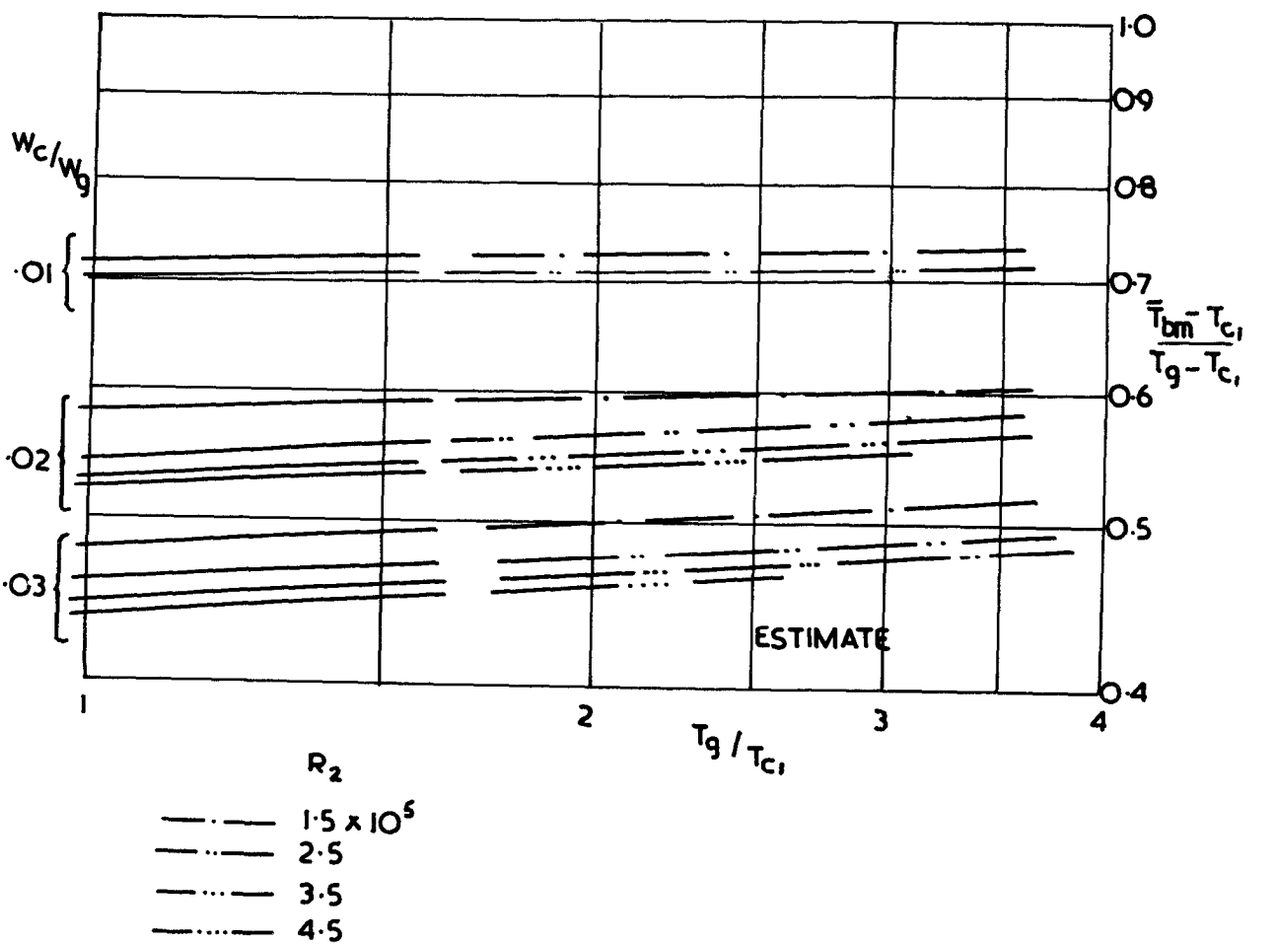

MIDSPAN MEAN SURFACE TEMPERATURE VARIATION WITH TEMPERATURE RATIO

FIG.10.

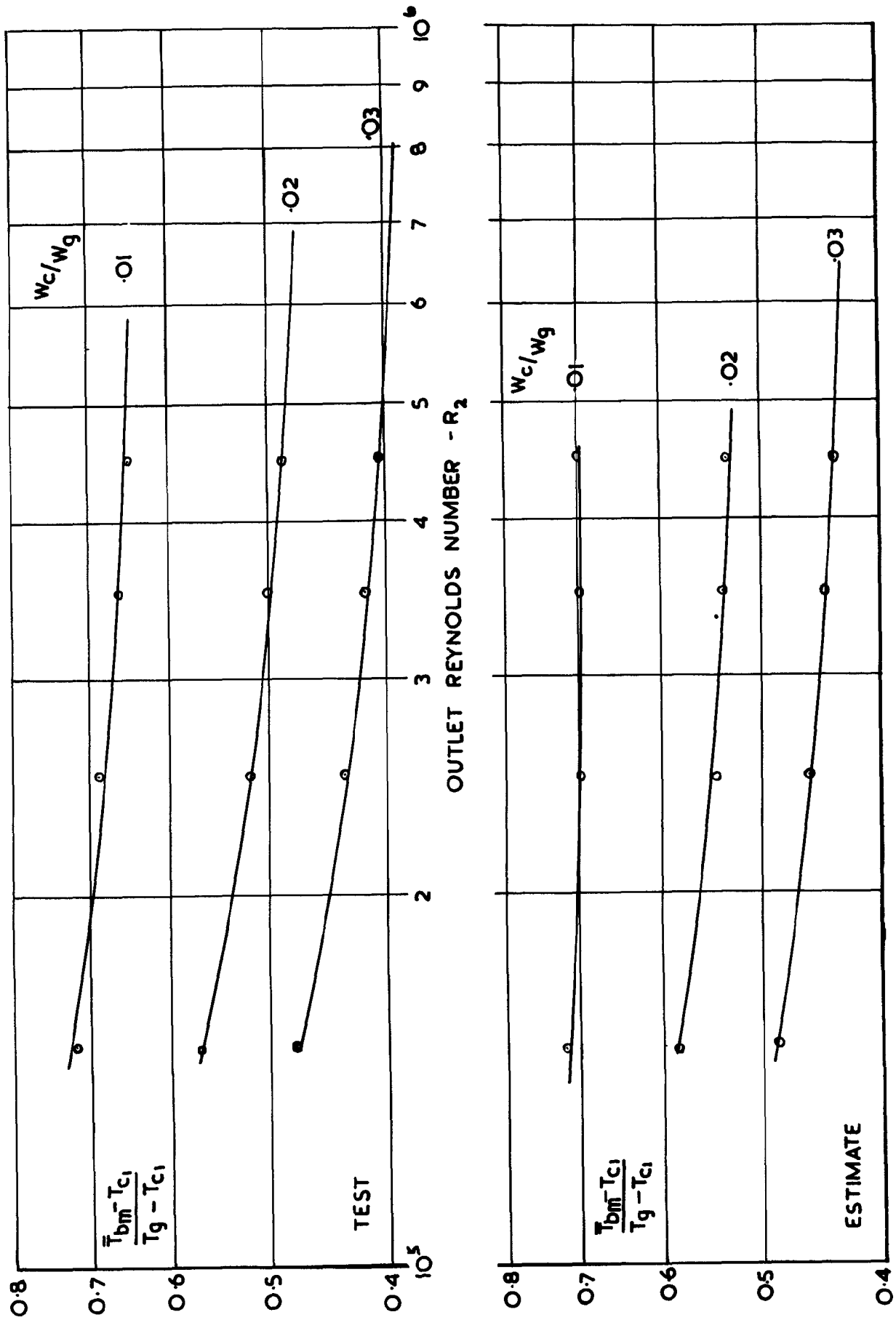

MIDSPAN MEAN SURFACE TEMPERATURES
FOR UNITY TEMPERATURE RATIO

FIG. 11.

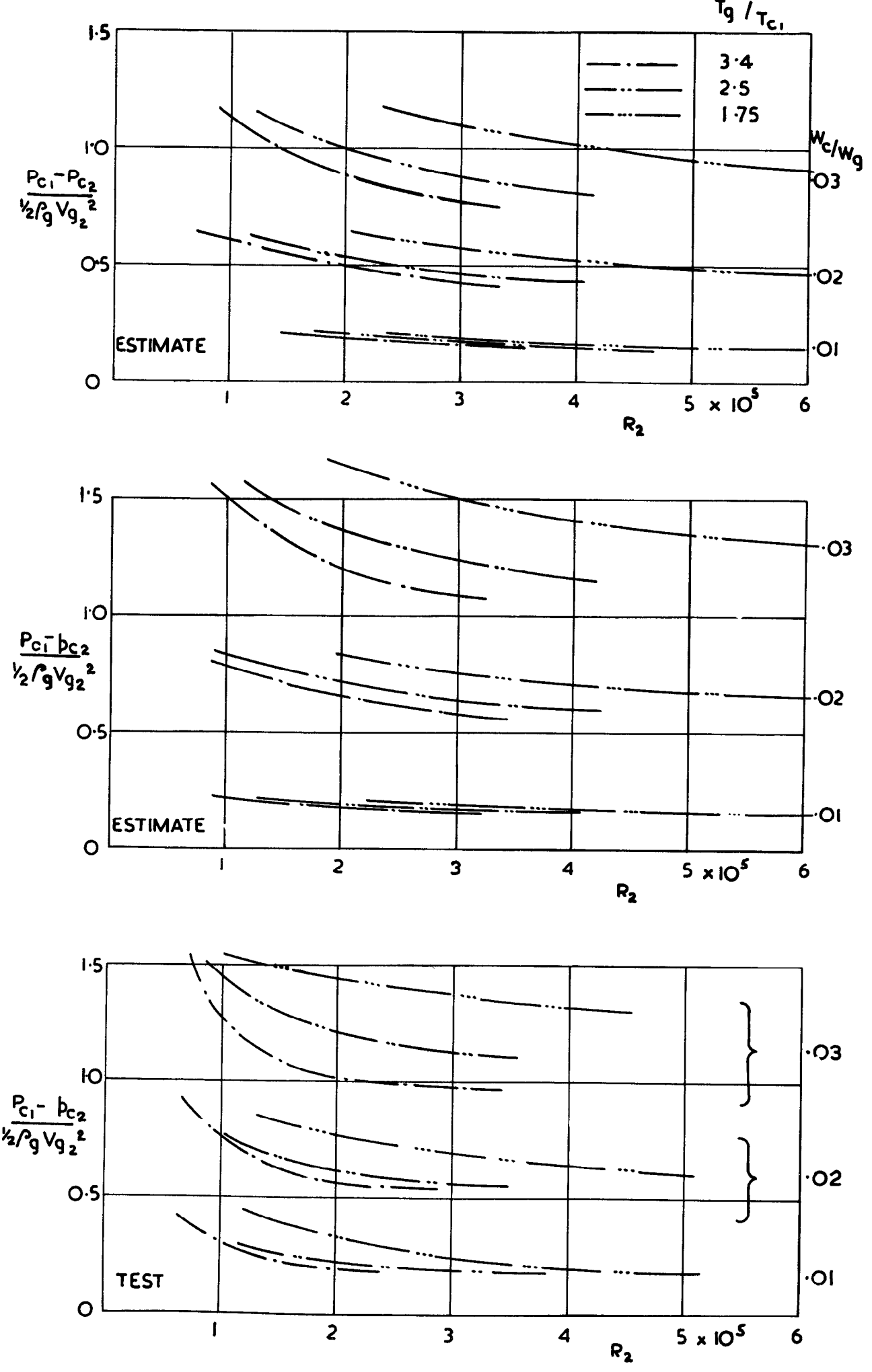

COOLANT PRESSURE DROP

C.P. No. 494
(20,477)
A.R.C. Technical Report

Printed and published by
HER MAJESTY'S STATIONERY OFFICE

To be purchased from
York House, Kingsway, London w.c.2
423 Oxford Street, London w.1
13A Castle Street, Edinburgh 2
109 St. Mary Street, Cardiff
39 King Street, Manchester 2
Tower Lane, Bristol 1
2 Edmund Street, Birmingham 3
80 Chichester Street, Belfast 1
or through any bookseller

Printed in England

S.O. Code No. 23-9011-94

C.P. No. 494